

An Inv(16)(p13.3q24.3)-Encoded *CBFA2T3-GLIS2* Fusion Protein Defines an Aggressive Subtype of Pediatric Acute Megakaryoblastic Leukemia

Tanja A. Gruber,^{1,6,8} Amanda Larson Gedman,⁶ Jinghui Zhang,^{2,8} Cary S. Koss,¹ Suresh Marada,³ Huy Q. Ta,⁶ Shann-Ching Chen,⁷ Xiaoping Su,^{2,25} Stacey K. Ogden,³ Jinjun Dang,⁶ Gang Wu,² Vedant Gupta,¹ Anna K. Andersson,⁶ Stanley Pounds,⁵ Lei Shi,⁵ John Easton,⁸ Michael I. Barbato,⁸ Heather L. Mulder,⁸ Jayanthi Manne,⁸ Jianmin Wang,^{4,8} Michael Rusch,^{2,8} Swati Ranade,²⁴ Ramapriya Ganti,⁶ Matthew Parker,² Jing Ma,⁷ Ina Radtke,⁶ Li Ding,^{8,11} Giovanni Cazzaniga,¹³ Andrea Biondi,¹⁴ Steven M. Kornblau,⁹ Farhad Ravandi,¹⁰ Hagop Kantarjian,¹⁰ Stephen D. Nimer,¹⁵ Konstanze Döhner,¹⁶ Hartmut Döhner,¹⁶ Timothy J. Ley,^{8,11,12} Paola Ballerini,¹⁷ Sheila Shurtleff,⁶ Daisuke Tomizawa,²⁰ Souichi Adachi,²¹ Yasuhide Hayashi,²² Akio Tawa,²³ Lee-Yung Shih,¹⁸ Der-Cherng Liang,¹⁹ Jeffrey E. Rubnitz,¹ Ching-Hon Pui,¹ Elaine R. Mardis,^{8,11,12} Richard K. Wilson,^{8,11,12} and James R. Downing^{6,8,*}

¹Department of Oncology

²Department of Computational Biology

³Department of Biochemistry

⁴Information Sciences

⁵Department of Biostatistics

⁶Department of Pathology

⁷Hartwell Center for Biotechnology and Bioinformatics

⁸St. Jude Children's Research Hospital, Washington University Pediatric Cancer Genome Project

St. Jude Children's Research Hospital, Memphis, TN 38105, USA

⁹Department of Blood and Marrow Transplantation

¹⁰Department of Leukemia

University of Texas MD Anderson Cancer Center, Houston, TX 77030, USA

¹¹The Genome Institute at Washington University

¹²Siteman Cancer Center

Washington University School of Medicine, St. Louis, MO 63110, USA

¹³Centro Ricerca Tettamanti, Pediatric Clinic, University of Milan-Bicocca, 20052 Monza, Italy

¹⁴Pediatric Unit, University of Milan-Bicocca, San Gerardo Hospital, 20900 Monza, Italy

¹⁵Molecular Pharmacology and Chemistry Program, Sloan Kettering Institute, New York, NY 10065, USA

¹⁶Department of Internal Medicine III, University of Ulm, 89081 Ulm, Germany

¹⁷Laboratoire d'Hématologie, Hôpital A. Trousseau, 75012 Paris, France

¹⁸Division of Hematology-Oncology, Department of Internal Medicine, Chang Gung Memorial Hospital, Chang Gung University, Taipei 105, Taiwan

¹⁹Division of Pediatric Hematology Oncology, Mackay Memorial Hospital, Taipei 104, Taiwan

²⁰Department of Pediatrics, Tokyo Medical and Dental University, Tokyo 113-8510, Japan

²¹Human Health Sciences, Graduate School of Medicine, Kyoto University, Kyoto 606-8501, Japan

²²Department of Haematology/Oncology, Gunma Children's Medical Center, Shibukawa 377-8577, Japan

²³Department of Pediatrics, National Hospital Organization Osaka National Hospital, Osaka 540-0006, Japan

²⁴Pacific Biosciences, Menlo Park, CA 94025, USA

²⁵Present address: Department of Bioinformatics and Computational Biology, University of Texas MD Anderson Cancer Center, Houston, TX 77030, USA

*Correspondence: james.downing@stjude.org

<http://dx.doi.org/10.1016/j.ccr.2012.10.007>

SUMMARY

To define the mutation spectrum in non-Down syndrome acute megakaryoblastic leukemia (non-DS-AMKL), we performed transcriptome sequencing on diagnostic blasts from 14 pediatric patients and validated our

Significance

Acute megakaryoblastic leukemia (AMKL) accounts for 10% of childhood acute myeloid leukemia (AML). Although AMKL patients with Down syndrome (DS-AMKL) have an excellent survival, non-DS-AMKL patients have an extremely poor outcome with a 3 year survival of less than 40%. With the exception of the t(1;22) seen in the majority of infants with non-DS-AMKL, little is known about the molecular lesions that underlie this leukemia subtype. Our results identified a fusion gene, *CBFA2T3-GLIS2*, that functions as a driver mutation in a subset of these patients. Importantly, pediatric patients with *CBFA2T3-GLIS2* expressing AMKL had inferior outcomes (5 year survival 34.3% versus 88.9%; $p = 0.03$), demonstrating that this lesion is a prognostic factor in this leukemia population.

findings in a recurrency/validation cohort consisting of 34 pediatric and 28 adult AMKL samples. Our analysis identified a cryptic chromosome 16 inversion (inv(16)(p13.3q24.3)) in 27% of pediatric cases, which encodes a CBFA2T3-GLIS2 fusion protein. Expression of CBFA2T3-GLIS2 in *Drosophila* and murine hematopoietic cells induced bone morphogenic protein (BMP) signaling and resulted in a marked increase in the self-renewal capacity of hematopoietic progenitors. These data suggest that expression of CBFA2T3-GLIS2 directly contributes to leukemogenesis.

INTRODUCTION

Acute megakaryoblastic leukemia (AMKL) accounts for approximately 10% of pediatric acute myeloid leukemia (AML) and 1% of adult AML (Athale et al., 2001; Barnard et al., 2007; Oki et al., 2006; Tallman et al., 2000). AMKL is divided into two subgroups: AMKL arising in patients with Down syndrome (DS-AMKL), and leukemia arising in patients without Down syndrome (non-DS-AMKL). Although DS-AMKL patients have an excellent prognosis with an ~80% survival, non-DS-AMKL patients do not fare as well, with a reported survival of only 14%–34% despite high-intensity chemotherapy (Athale et al., 2001; Barnard et al., 2007; Creutzig et al., 2005). With the exception of the t(1;22) seen in infant non-DS-AMKL, little is known about the molecular lesions that underlie this leukemia subtype (Carroll et al., 1991; Lion et al., 1992; Ma et al., 2001; Mercher et al., 2001).

We recently reported data from a high-resolution study of DNA copy number abnormalities (CNAs) and loss of heterozygosity on pediatric de novo AML (Radtko et al., 2009). These analyses demonstrated a very low burden of genomic alterations in all pediatric AML subtypes except AMKL. AMKL cases were characterized by complex chromosomal rearrangements and a high number of CNAs. To define the functional consequences of the identified chromosomal rearrangements in non-DS-AMKL, the St. Jude Children's Research Hospital-Washington University Pediatric Cancer Genome Project performed transcriptome and exome sequencing on diagnostic leukemia samples.

RESULTS

AMKL Is Characterized by Chimeric Transcripts

Transcriptome sequencing was performed on diagnostic leukemia cells from 14 pediatric non-DS-AMKL patients (discovery cohort) (see Tables S1 and S2 available online). Our analysis identified structural variations (SVs) that resulted in the expression of chimeric transcripts encoding fusion proteins in 12 of 14 cases (Table S3). Remarkably, in 7 of 14 cases, a cryptic inversion on chromosome 16 (inv(16)(p13.3q24.3)) was detected that resulted in the joining of *CBFA2T3*, a member of the ETO family of nuclear corepressors, to *GLIS2*, a member of the GLI family of transcription factors (Figures 1, 2, and S1). In six of these cases, exon 10 of *CBFA2T3* was fused to exon 3 of *GLIS2*, whereas in the remaining one case, exon 11 of *CBFA2T3* was fused to exon 1 of *GLIS2*. Both encoded proteins retain the three *CBFA2T3* N-terminal *nerf* homology regions that mediate protein interactions and the five *GLIS2* C-terminal zinc finger domains that bind the *Glis* DNA consensus sequence (Figures 1A and 1B). Whole-genome sequence analysis of tumor and germline DNA from four cases demonstrated that the

CBFA2T3-GLIS2 chimeric gene resulted from simple balanced inversions in three cases and a complex rearrangement involving chromosomes 16 and 9 in the fourth case (Figures 2 and S1).

Chimeric transcripts were also detected in five of seven leukemia samples that lacked expression of *CBFA2T3-GLIS2*, including one case each expressing in-frame fusions of *GATA2-HOXA9*, *MN1-FLI1*, *NIPBL-HOXB9*, *NUP98-KDM5A*, *GRB10-SDK1*, and *C8orf76-HOXA11AS* (Figure 3; Table S3). Importantly, several of the genes involved in these translocations play a direct role in normal megakaryocytic differentiation (*GATA2* and *FLI1*), have been previously shown to be involved in leukemogenesis (*HOXA9*, *MN1*, *HOXB9*, *NUP98*, *KDM5A*), or are highly expressed in hematopoietic stem cells or myeloid/megakaryocytic progenitors (Figure S2) (Argiropoulos and Humphries, 2007; Buijs et al., 2000; Heuser et al., 2011; Kawada et al., 2001; Visvader et al., 1995; Wang et al., 2009). Analysis of a recurrency/validation cohort consisting of diagnostic leukemia cells from 62 AMKL cases (34 pediatric and 28 adult) revealed 6 additional pediatric samples carrying *CBFA2T3-GLIS2* for an overall frequency of 27% (13 of 48) in pediatric AMKL (Table S1). None of the adult AMKL cases contained this chimeric transcript, suggesting that this lesion is restricted to pediatric non-DS-AMKLs. *NUP98-KDM5A* was the only other chimeric transcript that was recurrent, being detected in 8.3% (4 of 48) of pediatric cases (Table S1). This chimeric transcript was also not detected in adult AMKLs.

Cooperating Lesions in AMKL

In addition to the described chimeric transcripts, exome sequence analysis on 10 of the 14 samples in the discovery cohort that had matched germline DNA, coupled with CNAs detected by Affymetrix SNP6 microarrays, revealed an average of 5 (range 1–14) somatic nonsilent sequence mutations and 5 (range 0–11) CNAs involving annotated genes per case. (Tables S4, S5, and S6; Figure S1). Despite the relative paucity of somatic mutations, recurrent lesions were identified in *JAK* kinase genes, *MPL* and *GATA1*, which have been previously shown to play a role in AMKL (Malinge et al., 2008). Sequence analysis of these genes in cases within the recurrency cohort that had available genomic DNA revealed activating mutations in *JAK* kinases (9 of 51, 17.6%) and *MPL* (2 of 51, 3.9%), as well as inactivating mutations in *GATA1* (5 of 51, 9.8%) (Tables S1 and S6). In addition, 7 of 14 cases with available copy number data contained amplification of chromosome 21 in the Down syndrome critical region (DSCR; chr21q22) that includes genes known to play a role in AML such as *RUNX1*, *ETS2*, and *ERG* (Table S4; Figure S1). Three of these cases carry the *CBFA2T3-GLIS2* chimeric gene. Importantly, the total burden of somatic mutations was significantly lower in the *CBFA2T3-GLIS2*-expressing cases (7.17 ± 3.60 versus 16.60 ± 5.13 ; $p = 0.009$; Table S5).

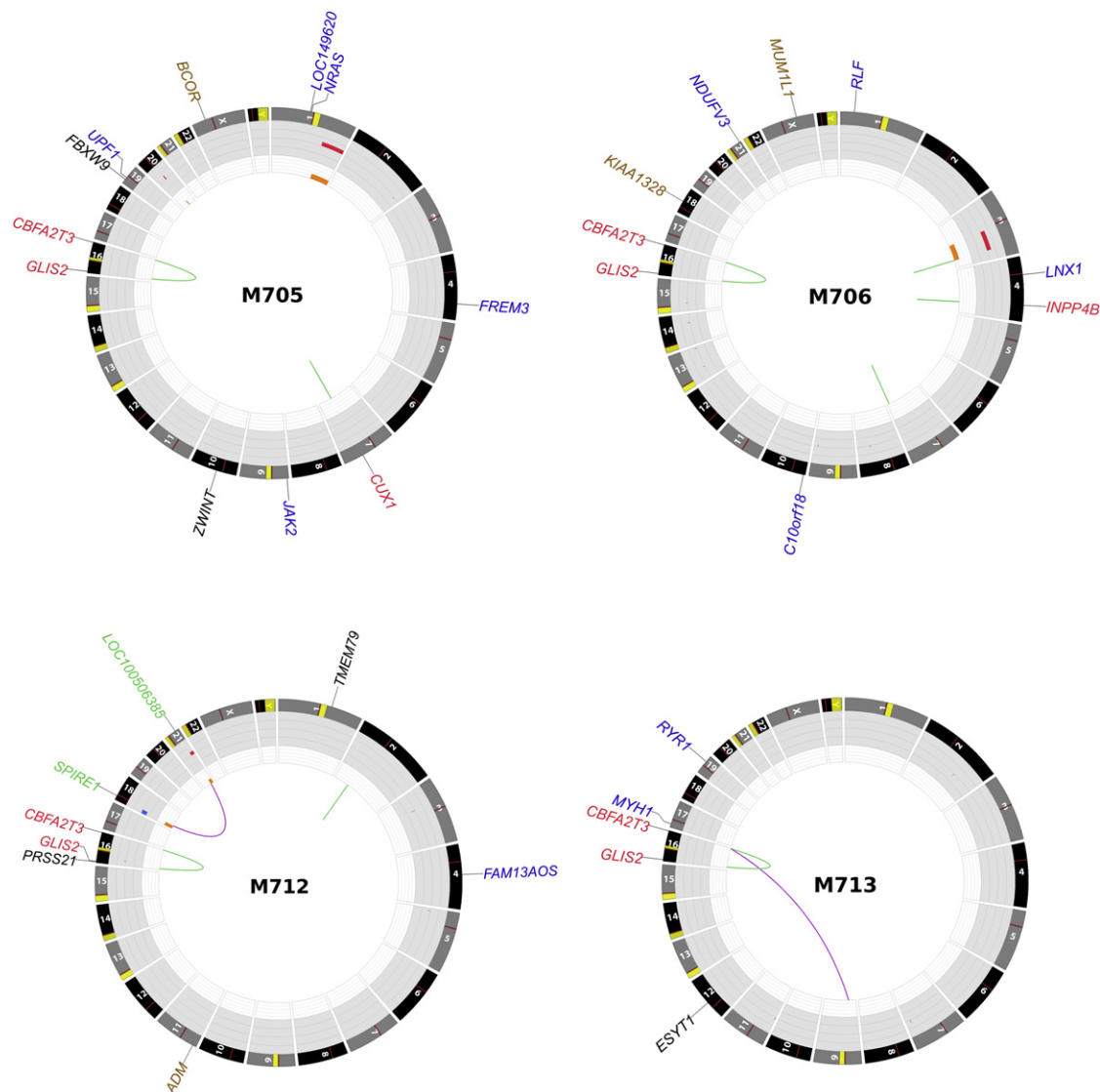


Figure 2. Somatic Mutations in Whole-Genome-Sequenced AMKL Cases

Plots depict structural genetic variants, including DNA copy number alterations, intra- and interchromosomal translocations, and sequence alterations (Krzywinski et al., 2009). DNA copy number alterations: loss of heterozygosity (LOH), orange; amplification, red; deletion, blue. Sequence mutations in Refseq genes: silent SNVs (SNVs), black; UTR, brown; nonsilent SNVs, blue. Genes at structural variant breakpoints: genes involved in in-frame fusions, red; others, green.

CBFA2T3-GLIS2-Modified Hematopoietic Cells Demonstrate Enhanced Self-Renewal

CBFA2T3 (also known as *MTG16*) was initially identified as a fusion partner with *RUNX1* in rare cases of therapy-related AML that contain a *t*(16;21)(q24;q22) (Gamou et al., 1998). More recently, *CBFA2T3* has been implicated in the maintenance of hematopoietic stem cell quiescence (Chyla et al., 2008). By contrast, to our knowledge, *GLIS2* has not been previously implicated in leukemogenesis. *GLIS2* is a member of the GLI-similar (*GLIS1-3*) subfamily of Krüppel-like zinc finger transcription factors and is closely related to the GLI family of transcription factors that function as critical elements of the hedgehog signaling pathway (Kim et al., 2007; Lamar et al., 2001). *GLIS2* is expressed in the kidney, and germline-inactivating mutations lead to nephronophthisis, an autosomal recessive

cystic kidney disease (Attanasio et al., 2007). Although *GLIS2* is not normally expressed in the hematopoietic system, its fusion to *CBFA2T3* as a result of the *inv*(16)(p13.3q24.3) results in high-level expression of the C-terminal portion of the protein including its DNA-binding domain (Figure S1).

To explore the functional effects of the *CBFA2T3*-*GLIS2* fusion protein, we transduced murine hematopoietic cells with a retrovirus expressing either *CBFA2T3*-*GLIS2* or *GLIS2* alone and assessed their effect on in vitro colony formation, differentiation, and replating efficiency as a surrogate measure of self-renewal (Figures 5A and 5B). On the initial plating, the expression of *CBFA2T3*-*GLIS2* had no effect on colony numbers, size, or overall myeloid/erythroid differentiation when cells were grown in the presence of IL3, IL6, SCF, and EPO. However, hematopoietic cells transduced with the empty

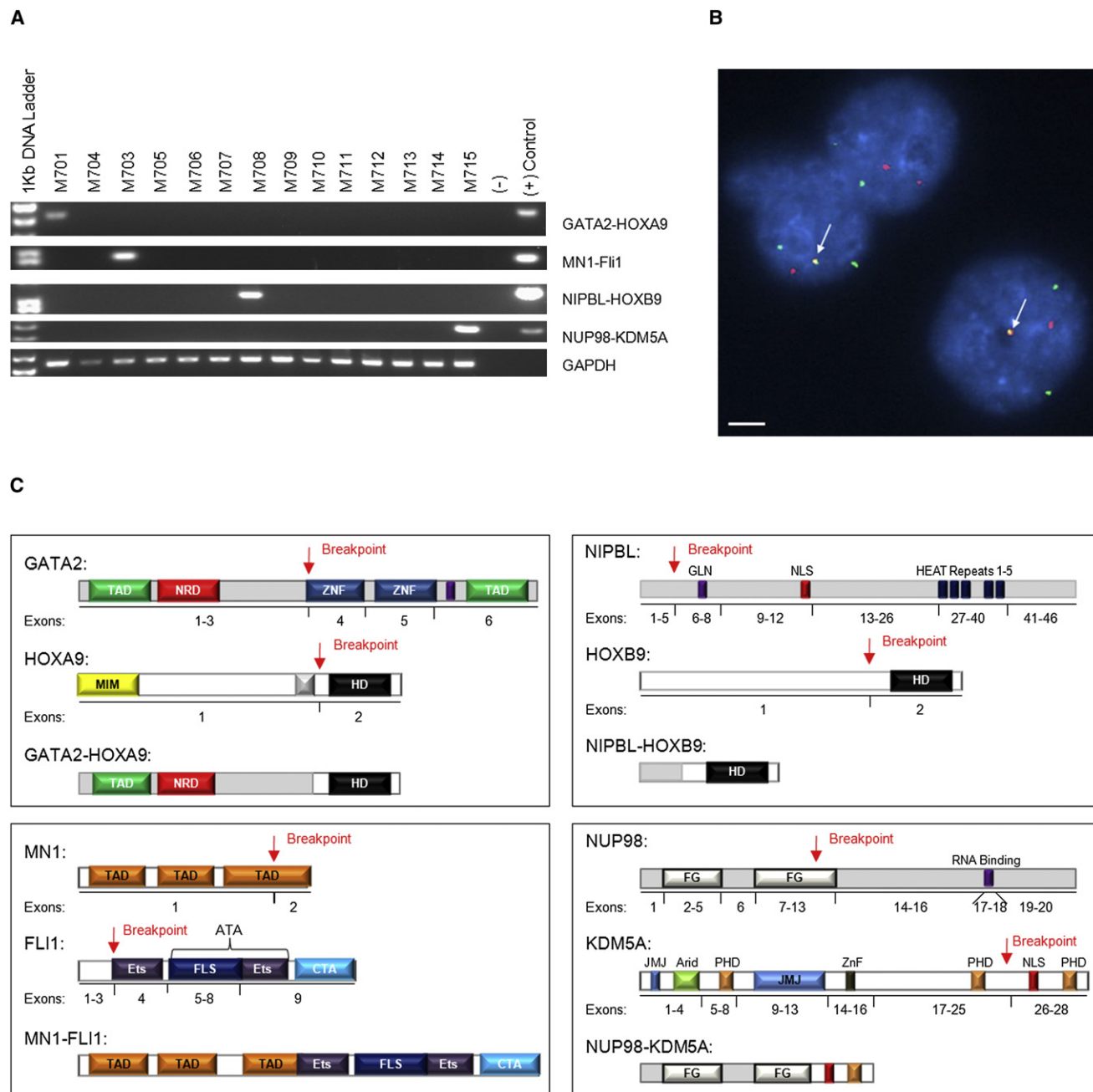


Figure 3. Low-Frequency Chimeric Transcripts in Pediatric AMKL

Four chimeric transcripts were identified in one case each of the discovery cohort and tested for in the recurrence cohort: *GATA2-HOXA9*, *MN1-FLI1*, *NIPBL-HOXB9*, and *NUP98-KDM5A*.

(A) RT-PCR validation of the discovery cohort. Primers and conditions are described in [Supplemental Experimental Procedures](#).

(B) Interphase FISH analysis of M703 carrying the *MN1-FLI1* chimeric protein. The *MN1* probe is red; the *FLI1* probe is green. White arrows indicate the fusion event. Scale bar, 10 μ m.

(C) Schematic of chimeric proteins. Exons and domains are not drawn to scale. NRD, negative regulatory domain; ZNF, zinc finger; MIM, Meis interaction motif; HD, Hox domain; Ets, E-twenty six domain; FLS, FLI1-specific region; CTA, C-terminal transactivation domain; GLN, glutamine-rich domain; NLS, nuclear-localizing signal; HEAT, Huntingtin/EF3/PP2A/TOR1 domain; FG, phenylalanine-glycine repeats; JMJ, jumonji domain; ARID, AT-rich interaction domain; PHD, plant homeodomain. See also [Figure S2](#).

retrovirus (MSCV-IRES-mCherry [MIC]) failed to form colonies after the second replating, whereas expression of either CBFA2T3-GLIS2 or wild-type GLIS2 resulted in a marked

increase in the self-renewal capacity, with colony formation persisting through ten replatings ([Figure 5C](#)). Upon serial replating, two colony types were detected: CFU-GM and CFU-Meg

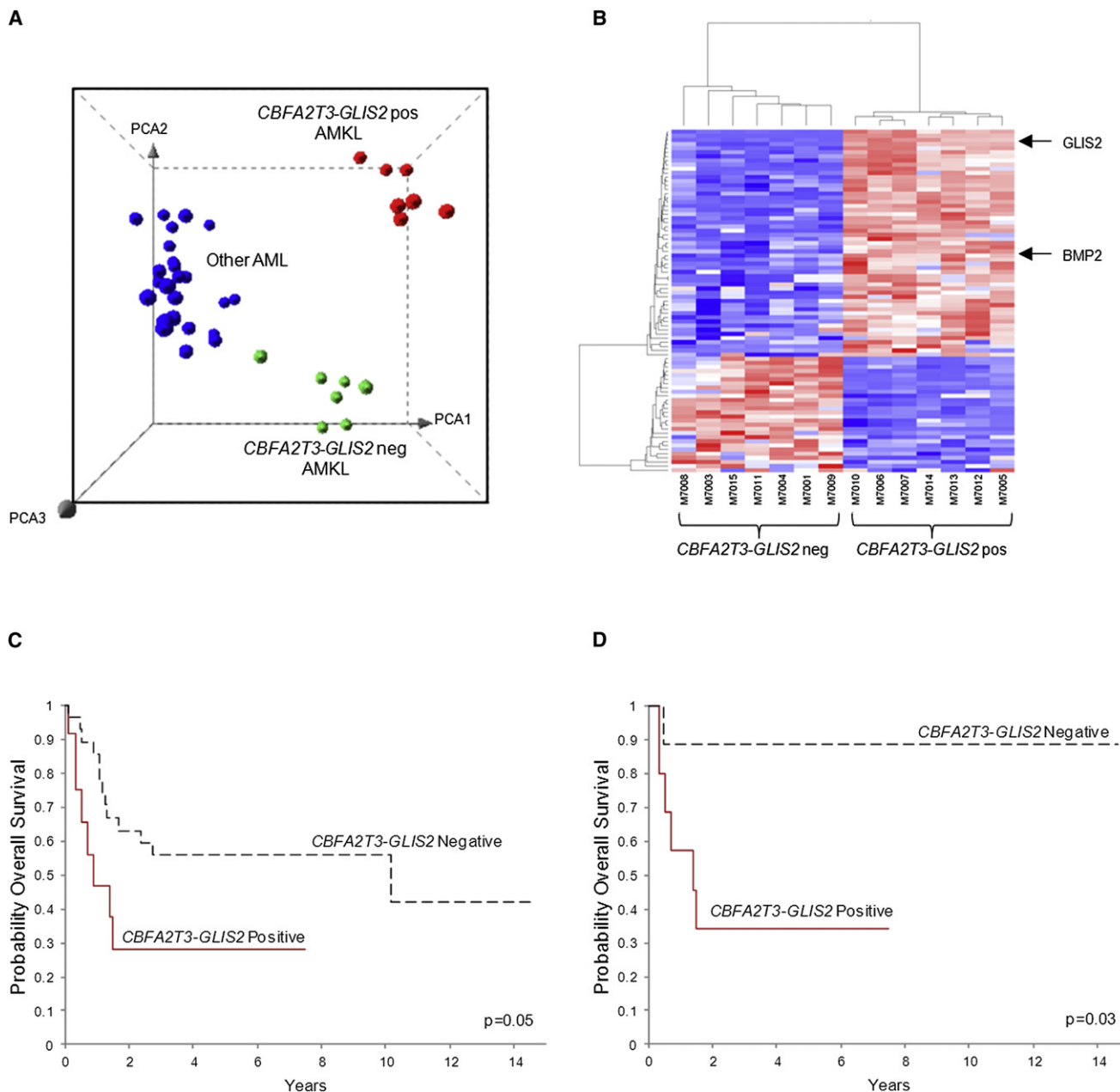


Figure 4. CBFA2T3-GLIS2 Defines a Unique Subtype of AML with a Distinct Gene Expression Signature and Poor Outcomes

(A) Principal component analysis of the gene expression profiles of the AMKL discovery cohort and 32 other non-AMKL AML samples representing all other known genetic subtypes of pediatric AML. Clusters were generated using 1,000 genes selected by k-means algorithm. A detailed description of the samples included in this analysis can be found at NCBI Gene Expression Omnibus, accession GSE35203.

(B) Heatmap of differentially expressed genes in the top-scoring network module of CBFA2T3-GLIS2-positive (pos) and -negative (neg) AMKL patient samples. For gene relationships, please see Figure S3. For a detailed list of the top 500 differentially expressed genes (not limited to this network), please see Table S7.

(C) Overall survival of 40 pediatric non-DS AMKL cases treated at multiple institutions (CBFA2T3-GLIS2-negative cases $n = 28$, and CBFA2T3-GLIS2-expressing cases, $n = 12$). The curves for the two groups were tested by log rank method and exact test using permutation that yielded a p value of 0.05.

(D) Overall survival of 19 pediatric non-DS AMKL cases treated at St. Jude Children's Research Hospital (CBFA2T3-GLIS2-negative cases, $n = 9$, and CBFA2T3-GLIS2-expressing cases, $n = 10$). The curves for the two groups were tested by log rank method and exact test using permutation that yielded a p value of 0.03. See also Figure S3 and Table S7.

(Figure 5D). Immunophenotypic analysis at the third replating also revealed evidence of megakaryocytic differentiation with CD41/CD61 dual expression and the absence of cKIT and

Sca1 expression in the majority of cells (Figure 5E). Importantly, CBFA2T3-GLIS2-expressing cells remained growth factor dependent, suggesting that cooperating mutations in growth factor

signaling pathways are likely required for full leukemic transformation (data not shown). Moreover, transplantation of *CBFA2T3-GLIS2*-transduced bone marrow cells into syngeneic recipients failed to induce overt leukemia at day 365 as demonstrated by normal blood counts and low-level reporter gene expression in peripheral blood (<5%) (data not shown), consistent with a requirement for cooperative mutations. Failure to induce leukemia in mice as a single lesion has been previously reported for other chimeric genes that confer the ability to serially replat in colony-forming assays, including *AML1-ETO* (Higuchi et al., 2002).

CBFA2T3-GLIS2 Induces BMP Signaling

GLIS2 can function as both a transcriptional activator and repressor depending on the cellular context and has been implicated in altered signaling through a number of pathways including sonic hedgehog-Gli1 (SHH) and WNT/ β -catenin (Attanasio et al., 2007; Kim et al., 2007). Analysis of the gene expression signatures of *CBFA2T3-GLIS2* expressing AMKLs revealed altered expression of a number of genes in the SHH and WNT pathways, as well as genes in the bone morphogenetic protein (BMP) pathway, which is directly influenced by SHH signaling (Figures 4B, 6A, and S3) (Dahn and Fallon, 2000; Ingham and McMahon, 2001; Vokes et al., 2007). When this analysis was limited to genes containing Gli consensus DNA-binding sites (Gli-BS) in their promoters or to genes known to be transcriptional targets of GLIS2, marked overexpression of *PTCH1*, *HHIP*, *BMP2*, and *BMP4* was observed (Figures 6B, S3, and S4; Table S7) (Attanasio et al., 2007). Consistent with this observation, although *CBFA2T3-GLIS2* only weakly activated transcription of a reporter construct containing the Gli-BS (Figure S4), it strongly activated transcription of the Gli-BS-containing *BMP4* promoter-driven luciferase construct and induced expression of *BMP4* in murine hematopoietic cells (Figures 6C and S4). Moreover, *CBFA2T3-GLIS2* strongly activated a BMP response element (BRE) containing luciferase reporter construct and induced expression of the BMP downstream transcriptional target, inhibitor of differentiation 1 (*Id1*) (Korchynskyi and ten Dijke, 2002), consistent with the induced expression of *BMP2*/*BMP4* (Figure S4).

BMP signaling plays a critical role in the specification of hematopoiesis in developing embryos, and studies suggest that *BMP4* stimulation can augment megakaryocytic output from CD34 progenitors (Jeanpierre et al., 2008; Söderberg et al., 2009). To determine if the observed *CBFA2T3-GLIS2*-induced BMP expression contributes to the enhanced replating capacity of murine hematopoietic cells, colony-replating assays were repeated in the presence of dorsomorphin, a selective small molecule inhibitor of the BMP type I receptors that blocks BMP-mediated phosphorylation of SMAD 1/5/8 (Yu et al., 2008). Importantly, *CBFA2T3-GLIS2* as well as *GLIS2*-expressing hematopoietic cells were significantly more sensitive to dorsomorphin than wild-type cells in the first plating (Figure 6D). Continuous exposure to dorsomorphin inhibited colony formation in a dose-dependent manner on subsequent platings (data not shown). Interestingly, sublethal doses of dorsomorphin in *CBFA2T3-GLIS2*-positive cells led to an upregulation of *Bmp4* and *Id1* transcripts over time, with colony counts returning to untreated levels, suggesting that cells are able to overcome

this inhibition by upregulating the BMP pathway (data not shown).

To further explore the downstream signaling of *CBFA2T3-GLIS2* in human leukemia cell lines, we first assessed the expression level of *GLIS2* in human cancer cell lines using the recently published Broad-Novartis Cancer Cell Line Encyclopedia (Figure 7A) (Barretina et al., 2012). Interestingly, this analysis showed that *GLIS2* expression levels are lowest in leukemia cell lines. Moreover, within the leukemias, the highest expressing cell line was the pediatric AMKL cell line M07e. To further explore AMKL cell lines, we performed RT-PCR for *CBFA2T3-GLIS2* on five human AMKL cell lines. Three of the five cell lines (RS1, WSU-AML, and M07e) expressed *CBFA2T3-GLIS2* (Figure 7B). The presence of the chimeric gene in these lines was validated by FISH analysis (Figure 7B). We went on to determine the relative expression of BMP genes by semiquantitative RT-PCR and found a trend toward upregulation of these genes in the *CBFA2T3-GLIS2*-positive cells (Figure 7C). We also assessed our AMKL cell lines for dorsomorphin sensitivity and found a trend toward increased sensitivity in cell lines expressing *CBFA2T3-GLIS2* as determined by a standard MTT assay (Figure 7D).

To determine if *CBFA2T3-GLIS2* induces the upregulation of BMP signaling in vivo, we generated transgenic *Drosophila* expressing either *CBFA2T3-GLIS2* or full-length *GLIS2* using an epithelial promoter and examined their effect on fly development. During *Drosophila* development, the WNT, BMP, and SHH homologs (Wg, Dpp, and Hh, respectively) have distinct roles in patterning adult wing structures (Dahn and Fallon, 2000; Ingham and McMahon, 2001; Vokes et al., 2007). When altered, these signaling pathways trigger characteristic loss- and gain-of-function phenotypes (Tabata and Takei, 2004). Expression of *CBFA2T3-GLIS2* and full-length *GLIS2* in *Drosophila* resulted in ectopic expression of endogenous *dpp*, the fly homolog of *BMP4*, in wing imaginal discs (Figures 8A and S5). Immunofluorescence confirmed the nuclear localization of *CBFA2T3-GLIS2* (Figure 8A). Both *CBFA2T3-GLIS2* and *GLIS2* overexpression induced lethality. However, a small number of escapers developed to pharate adults and demonstrated a morphologic *dpp* gain-of-function phenotype; wing hinges were converted to notum, and legs were shortened and broadened (Figure 8B) (Grieder et al., 2009). Rare *CBFA2T3-GLIS2* transgenic flies developed to adulthood and demonstrated mild ectopic venation throughout the wing blade, as well as wing blistering consistent with a *dpp* gain-of-function phenotype (Figure 8B) (Sander et al., 2010).

DISCUSSION

Sequence analysis of pediatric non-DS-AMKLs revealed the expression of an inv(16)-encoded *CBFA2T3-GLIS2* in almost 30% of pediatric non-DS-AMKL patients, and its presence defined a distinct subgroup of patients that had an exceptionally poor outcome when compared to patients with AMKL that lacked this lesion. In addition, five other chimeric transcripts (*GATA2-HOXA9*, *MN1-FLI1*, *NIPBL-HOXB9*, *GRB10-SDK1*, and *C8orf76-HOXA11AS*) were detected in single AMKL cases. Surprisingly, none of the identified chimeric transcripts was detected in adult AMKL cases, highlighting the significant

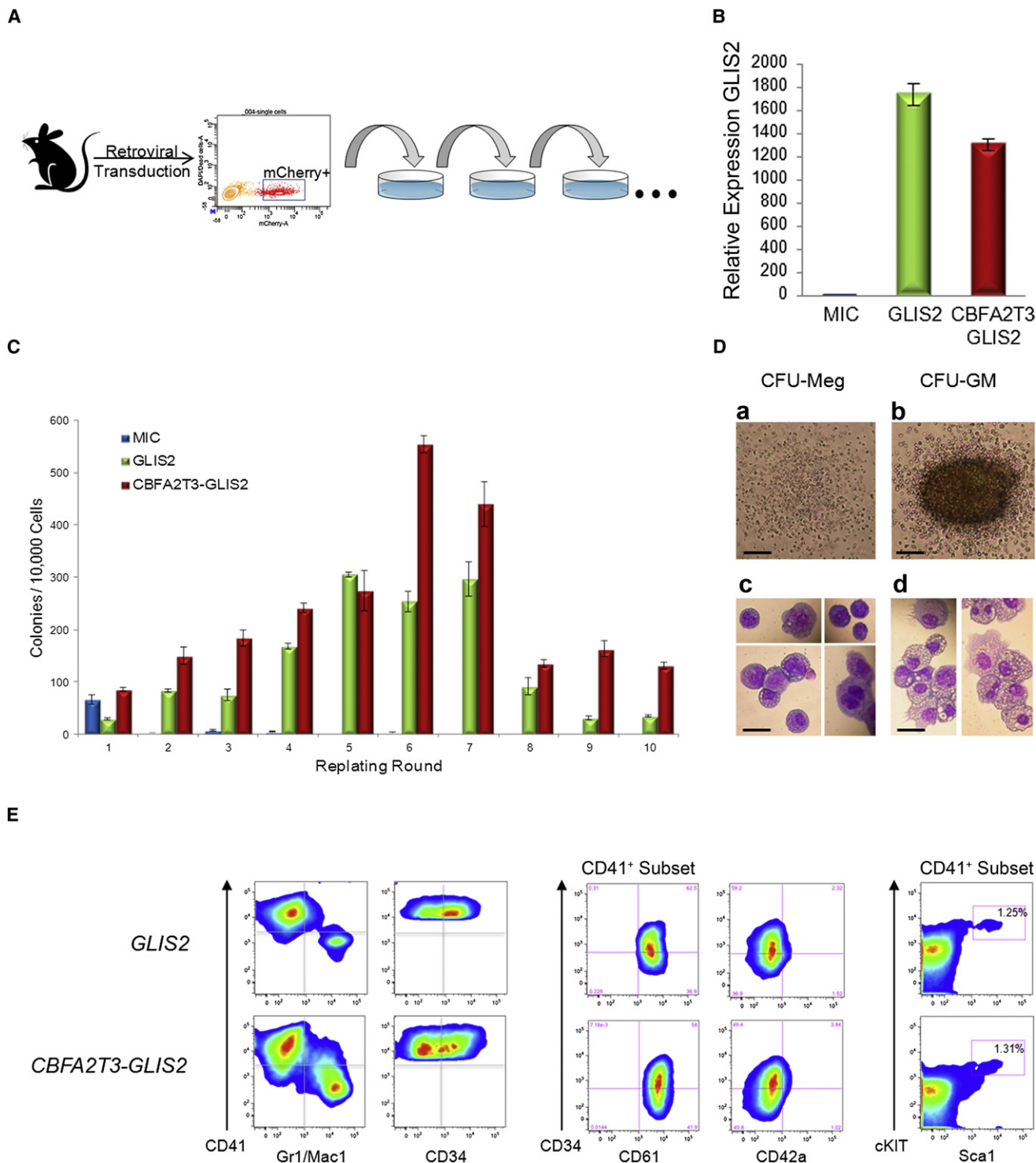


Figure 5. CBFA2T3-GLIS2 Leads to Enhanced Replating of Hematopoietic Cells

(A) Experimental design. Murine bone marrow cells were transduced with retroviral vectors expressing mCherry alone (MIC), or mCherry along with *GLIS2*, or *CBFA2T3-GLIS2*. Transduced cells were purified by sorting mCherry-positive cells and plated onto methylcellulose containing IL3, IL6, SCF, and EPO. Colonies were counted after 7 days of growth and replated serially.

(B) Semiquantitative RT-PCR of *GLIS2* utilizing cells harvested from first round of plating. *GLIS2* primers are specific for the 3' half of the transcript and thus pick up both full-length *GLIS2* as well as *CBFA2T3-GLIS2*. Expression in MIC cells was defined as one (1), and data are pooled from two separate experiments with similar results. $p \leq 0.0001$ as determined by one-way ANOVA. Error bars represent mean \pm SEM of two independent experiments.

(C) Number of colonies detected at 7 days following each plating. Error bars represent mean \pm SEM of two independent experiments.

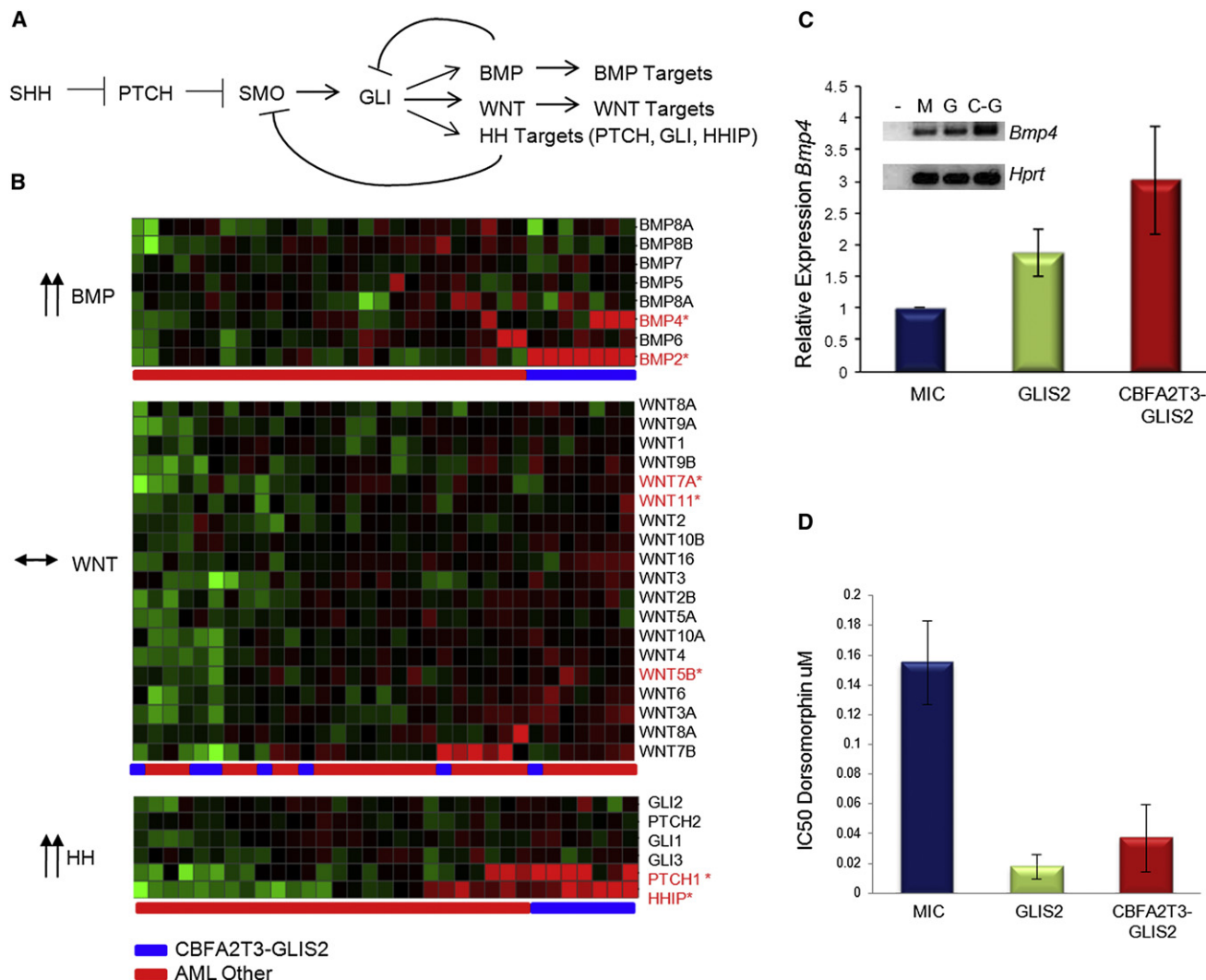


Figure 6. CBFA2T3-GLIS2 Activates the BMP Pathway

(A) The Hedgehog (HH) signaling pathway. In addition to classic hedgehog targets such as *PTCH* and *HHIP*, *WNT* and *BMP* gene expression have been demonstrated to be affected by the GLI transcription factor in various models (Dahn and Fallon, 2000; Ingham and McMahon, 2001; Vokes et al., 2007).

(B) Gene expression profiles from *CBFA2T3-GLIS2* containing AMKL cases and other AML subtypes were evaluated for expression levels of *BMP*, *WNT*, and *HH* target genes. *CBFA2T3-GLIS2*-negative AMKL cases are not shown in this analysis. Significantly upregulated probe sets (FDR less than 0.05) are designated with red font: *BMP2* FDR 1.06×10^{-17} , *BMP4* FDR 0.015976, *PTCH1* FDR 2.05×10^{-6} , and *HHIP* FDR 0.0038.

(C) Murine bone marrow cells were transduced with retroviral vectors carrying mCherry alone (MIC), mCherry plus *GLIS2*, or *CBFA2T3-GLIS2*. mCherry-positive cells were sorted and plated in methylcellulose containing IL3, IL6, SCF, and EPO. Following 1 week of growth, RNA was isolated, reverse transcribed, and amplified with *Bmp4* or *Hprt*-specific primers. Error bars represent mean \pm SEM of four independent experiments. A representative gel is shown (–, neg; M, MIC; G, *GLIS2*; C-G, *CBFA2T3-GLIS2*). $p = 0.047$ as determined by one-way ANOVA.

(D) *GLIS2* and *CBFA2T3-GLIS2* sensitize murine hematopoietic cells to BMP receptor type I inhibition. Colony-formation assays were conducted in the presence or absence of dorsomorphin at the indicated concentrations (Yu et al., 2008). IC₅₀ values were calculated as the amount of drug required to inhibit 50% of the colony formation as determined by colony counts. Error bars represent mean \pm SEM of two independent experiments. $p = 0.036$ as determined by one-way ANOVA. See also Figure S4.

biological differences between pediatric and adult AMKL. Importantly, each of the detected chimeric transcripts is predicted to encode a fusion protein that would alter signaling pathways

known to play a role in normal hematopoiesis, suggesting that these lesions are “driver” mutations that directly contribute to the development of leukemia. In addition to these somatic

(D) Colony morphology detected in *GLIS2* and *CBFA2T3-GLIS2*-modified cells from the second plating and beyond. a, CFU-Meg; b, CFU-GM. Scale bars, 500 μ m. Representative cytopins and morphology of each colony type are shown. c, CFU-Meg; d, CFU-GM. Scale bars, 50 μ m.

(E) Cells harvested from colony-forming assays after three or more replatings were subjected to flow cytometry. Cells were negative for acetylcholinesterase (data not shown).

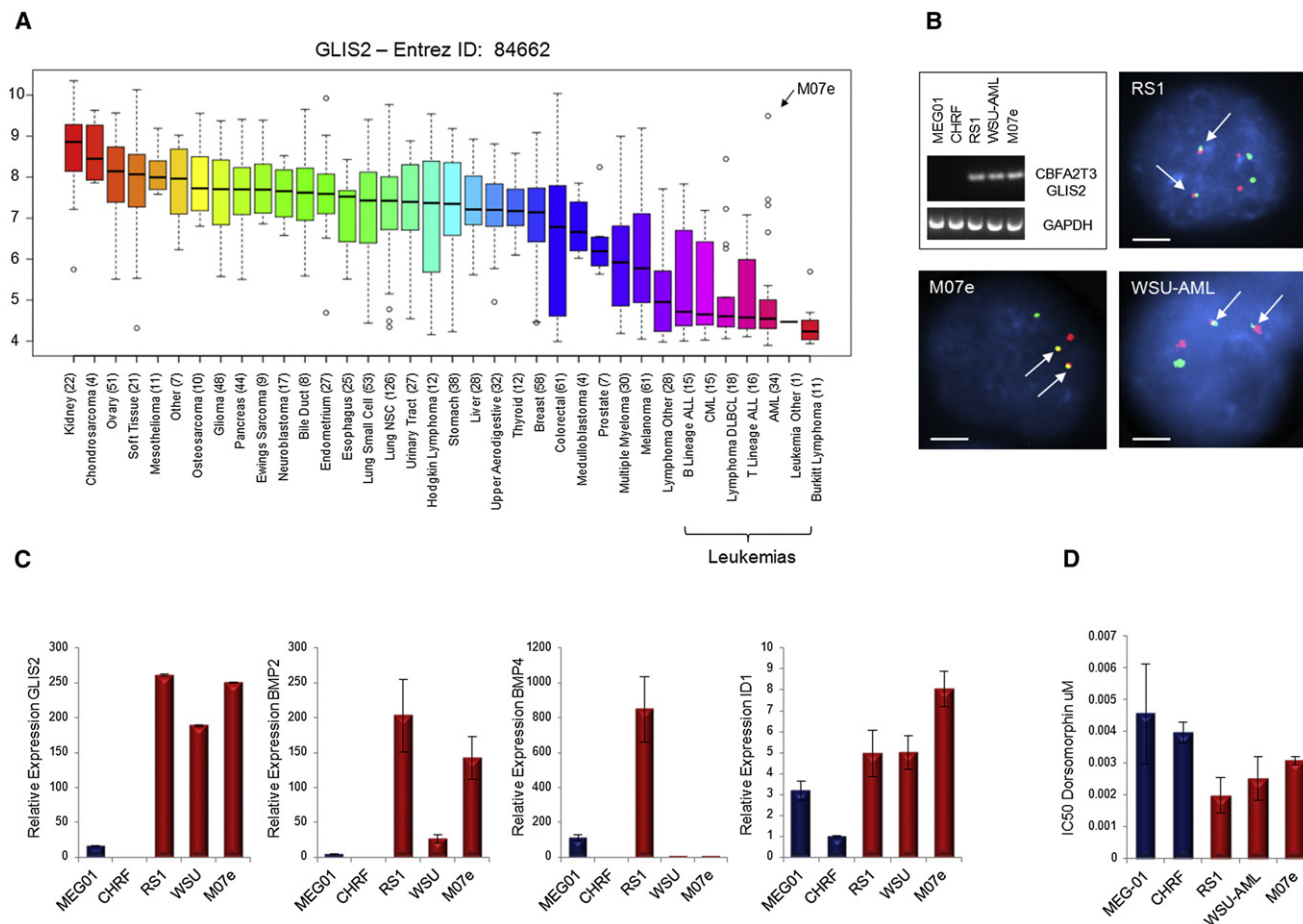


Figure 7. CBFA2T3-GLIS2 Is Present in AMKL Cell Lines

(A) *GLIS2* expression as determined by gene expression arrays in 991 human cancer cell lines. \log_2 -transformed expression levels are shown. Data were obtained from the Broad-Novartis Cancer Cell Line Encyclopedia (<http://www.broadinstitute.org/ccle/home>). A total of 34 AML cell lines are included; the extreme outlier of this subtype, M07e, is indicated. The *GLIS2* probe set recognizes the end of the transcript and thus does not distinguish between wild-type *GLIS2* and *CBFA2T3-GLIS2*. Median values are indicated by the band within the box plots; the ends of the whiskers indicate upper and lower adjacent values. Outliers are denoted by open circles.

(B) RT-PCR on five AMKL cell lines: MEG-01, CHRF-288-11, RS-1, WSU-AML, and M07e. The three cell lines carrying *CBFA2T3-GLIS2* were validated by FISH. Scale bars, 10 μ m.

(C) Real-time semiquantitative RT-PCR of *GLIS2*, *BMP2*, *BMP4*, and *ID1* on the five AMKL cell lines. Expression levels relative to β -actin are shown. CHRF-288-11 expression levels were set to one (1) for comparison across cell lines. Error bars represent mean \pm SEM of two independent experiments.

(D) Dorsomorphin sensitivity in the cell lines as determined by MTT assay. Error bars represent mean \pm SEM of two independent experiments. For cell line information and MTT assay, please see Supplemental Experimental Procedures.

structural alterations, a variety of other somatic mutations were detected, including activating mutations in kinase signaling pathways in 21.6% of cases (*JAK* kinase family members and *MPL*), inactivating mutations in *GATA1* in 9.8% of cases, and amplification of chromosome 21 in the DSCR that includes genes known to play a role in AML such as *RUNX1*, *ETS2*, and *ERG* in 50% of the cases. How these mutations interact to not only induce overt leukemia but also to influence therapeutic responses remains to be determined.

As part of the St. Jude Children's Research Hospital-Washington University Pediatric Cancer Genome Project, we have sequenced 260 cases of pediatric cancers across multiple tumor types (Downing et al., 2012). The *CBFA2T3-GLIS2* fusion was limited to AMKL cases. This specificity may exist for several

reasons. The N-terminal portion of the fusion, *CBFA2T3*, is primarily expressed in the hematopoietic compartment, leading one to predict that expression of the inversion product, if it were to occur, would primarily be limited to hematopoietic cells. Although we do not know the exact target cell of transformation, induction of *BMP4* signaling in human CD34⁺ progenitors has been demonstrated to increase the percentage of megakaryocyte and erythroid colonies in vitro (Fuchs et al., 2002; Jeanpierre et al., 2008). Thus, enhanced *BMP* signaling as a result of the expression of the inv(16)-encoded *CBFA2T3-GLIS2* may directly contribute to the megakaryocytic differentiation of the leukemia cells.

The inv(16)-encoded *CBFA2T3-GLIS2* chimeric gene induced aberrant high-level expression of the DNA-binding domain of

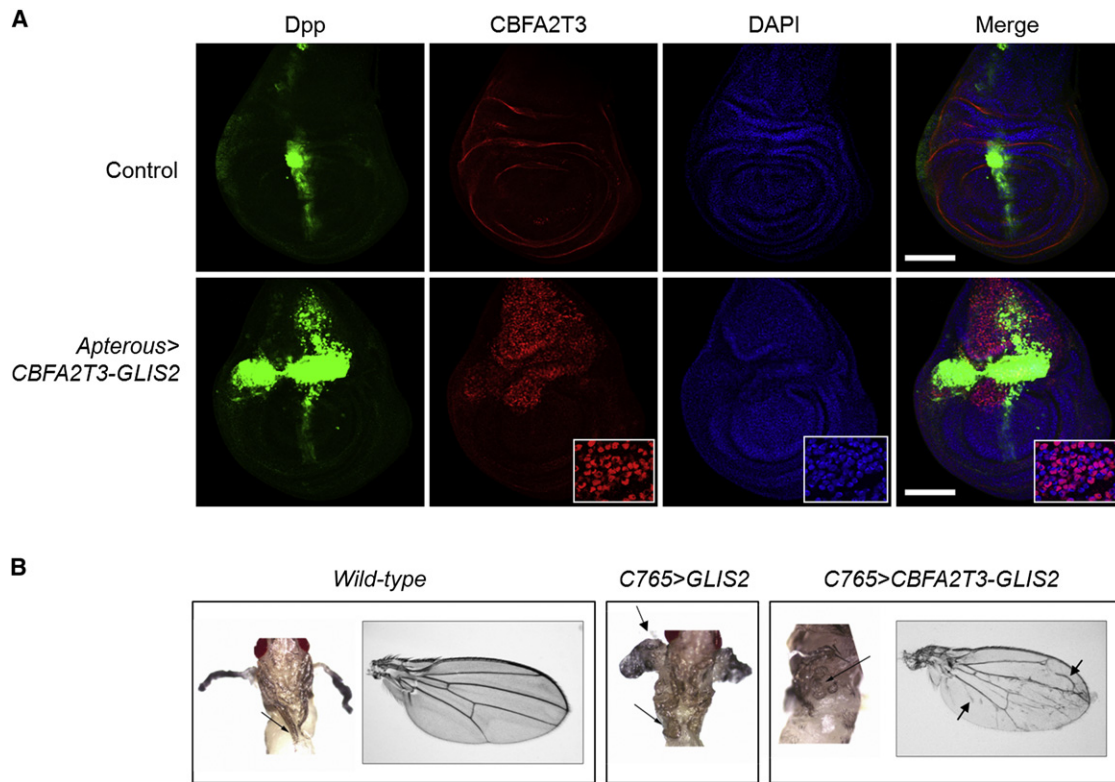


Figure 8. Transgenic *CBFA2T3-GLIS2* *Drosophila* Ectopically Expresses Dpp

(A) *CBFA2T3-GLIS2* was expressed under control of *Apterous-Gal4* (strong epithelial dorsal driver). *dpp-lacZ* serves as a reporter for *dpp* induction. Wing imaginal discs were isolated at the late third instar, stained for β -gal as a readout for *dpp* (green), *CBFA2T3* (red), and DAPI (blue), followed by immunofluorescence analysis. Nuclear localization of *CBFA2T3-GLIS2* can be seen by the pink signal (inset). Scale bars, 100 μ m.

(B) *CBFA2T3-GLIS2* was expressed under control of *C765*, a weak epithelial driver. Pharate adults were dissected from pupal casings and imaged. Arrows indicate ectopic notum, broadened and shortened legs. No *C765 > GLIS2* *Drosophila* matured to adulthood. Arrows indicate ectopic veins in wings of rare *C765 > CBFA2T3-GLIS2* escapers.

See also Figure S5.

GLIS2 in hematopoietic cells, along with the disruption of one allele of *CBFA2T3*, a gene whose encoded protein has been shown to play a role in maintaining normal hematopoietic stem cell quiescence (Chyla et al., 2008). GLIS2 is a distant member of the GLI superfamily of transcriptional factors that function as critical transcriptional targets of the SHH signaling pathway (Hui and Angers, 2011). Although alterations in the SHH pathway have been directly implicated in a range of cancers (Barakat et al., 2010), the role of SHH signaling in normal hematopoiesis and leukemia remains poorly defined (Lim and Matsui, 2010). Our data suggest that aberrant expression of GLIS2 results in upregulation of the classic SHH-negative feedback inhibitors PTCH and HHIP, coupled with a marked increase in the expression of BMP 2 and 4, resulting in enhanced BMP signaling. These results indicate that *CBFA2T3-GLIS2* functions, in part, as a gain-of-function GLIS2 allele. The exact mechanisms by which GLIS2 induced the upregulation of BMP2/BMP4 remains incompletely defined, although our data suggest that a direct transcription effect of GLIS2 on the BMP4 promoter is likely, although an indirect mechanism may also contribute.

Interestingly, BMP4 has been shown to expand and maintain human cord blood hematopoietic stem cells in vitro both directly, as well as indirectly via SHH signaling (Bhardwaj et al., 2001;

Bhatia et al., 1999). Furthermore, *ID1*, a downstream BMP target previously implicated in leukemogenesis, was found to be upregulated in *CBFA2T3-GLIS2*-modified hematopoietic cells, demonstrating that this pathway is activated (Wang et al., 2011). Consistent with these findings, we demonstrated that activation of BMP signaling contributed to the marked increase in the replating capacity of myeloid/erythroid-committed progenitors. Accordingly, we found that murine hematopoietic cells carrying either full-length *GLIS2*, or *CBFA2T3-GLIS2*, demonstrated an increased sensitivity to BMP inhibition, suggesting that upregulation of this pathway contributes to the observed phenotype. In addition, BMP4 signaling has been shown to induce the differentiation of human CD34+ progenitors into megakaryocytes (Jeanpierre et al., 2008), suggesting that the upregulation of this pathway is also contributing to the megakaryocyte differentiation phenotype of these leukemias. Finally, BMP4, like thrombopoietin, appears to exert its effects on human megakaryopoiesis in part through the JAK/STAT pathways (Jeanpierre et al., 2008). Interestingly, functional pathway analysis of gene expression profiles in *CBFA2T3-GLIS2*-positive AMKL samples identified genes in the Jak-STAT signaling pathway to be significantly upregulated ($p = 0.0038$; FDR 0.022978; Figure S4). Combined with the identification in some cases of

activating mutations in either JAK family members or MPL in *CBFA2T3-GLIS2*-expressing leukemias, our data suggest that these lesions likely cooperate in leukemogenesis.

Taken together, these data define a poor prognostic subgroup of pediatric AMKL patients that are characterized by the inv(16)(p13.3q24.3)-encoded *CBFA2T3-GLIS2* fusion protein. Expression of *CBFA2T3-GLIS2* induces an enhanced replating capacity of lineage-committed myeloid progenitors, along with megakaryocytic differentiation, in part through enhanced BMP2/BMP4 signaling. Whether altered SHH and *CBFA2T3*-induced signaling also contributes to leukemogenesis remains to be determined. Nevertheless, the presented data raise the important possibility that inhibition of the BMP pathway may have a therapeutic benefit in this aggressive form of pediatric AML.

EXPERIMENTAL PROCEDURES

Patients and Samples

Paired-end transcriptome sequencing on diagnostic leukemic blasts was performed on 14 pediatric non-DS-AMKL cases using the Illumina platform. Four of these cases underwent whole-genome sequencing (WGS) on diagnostic leukemia blasts and matched germline samples. All 14 cases underwent whole-exome sequencing for which 10 had matching germline samples. One additional diagnostic sample with matched germline DNA had whole-exome sequencing done that did not undergo transcriptome sequencing. All 15 of these patients were treated at St Jude Children's Research Hospital from 1990 to 2008. The recurrence cohort consisted of 61 additional cases including 33 pediatric specimens and 28 adult specimens. All samples were obtained with patient or parent/guardian-provided informed consent under protocols approved by the Institutional Review Board at each institution and St. Jude Children's Research Hospital.

Sequencing

RNA and DNA library construction for transcriptome and whole-genome DNA sequencing, respectively, has been described previously (Mardis et al., 2009; Zhang et al., 2012). Analysis of WGS data and whole-exome sequencing data that include mapping, coverage and quality assessment, single-nucleotide variant (SNV)/indel detection, tier annotation for sequence mutations, prediction of deleterious effects of missense mutations, and identification of loss of heterozygosity was described previously (Zhang et al., 2012). Please see Supplemental Experimental Procedures for details.

Recurrency Screening for Sequence Variations and Fusions

We performed recurrence screening on a cohort of 61 AMKL samples. All 61 were screened by RT-PCR (see Supplemental Experimental Procedures for primers and conditions) for *CBFA2T3-GLIS2*, *GATA2-HOXA9*, *MN1-FLI1*, *NIPBL-HOXB9*, and *NUP98-KDM5A*. Whole-genome-amplified DNA (QIAGEN) from 38 cases underwent PCR and Sanger sequencing by Beckman Coulter Genomics for *JAK1*, *JAK2*, *JAK3*, and *MPL* mutations. In 8 of 38 cases, a paired matched germline was available. Putative SNVs and indel variants were detected by SNPdetector (Zhang et al., 2005).

Overall Survival Probabilities

Outcome data were available for 40 pediatric patients tested for *CBFA2T3-GLIS2*. *CBFA2T3-GLIS2* was found in 13 patients. Overall survival was defined as the date of diagnosis or study enrollment to the date of death with surviving patients censored at the date of last follow-up. Survival curves were estimated using the Kaplan-Meier method and compared using the exact log rank test based on 10,000 permutations.

Affymetrix SNP Array

Affymetrix SNP 6.0 array genotyping was performed for 14 of 15 AMKL cases in the discovery cohort, and array normalization and DNA copy number alterations were identified as previously described (Lin et al., 2004; Mullighan et al.,

2007; Olshen et al., 2004; Pounds et al., 2009). To differentiate inherited copy number alterations from somatic events in leukemia blasts from patients lacking matched normal DNA, identified putative variants were filtered using public copy number polymorphism databases and a St. Jude database of SNP array data from several hundred samples (Iafate et al., 2004; McCarroll et al., 2008).

Gene Expression Profiling

Gene expression profiling was performed using Affymetrix Human Exon 1.0 ST Arrays (Affymetrix) according to manufacturer's instructions. This cohort comprised 39 pediatric AML samples including AMKL (n = 14), *AML1-ETO* (n = 4), *CBFB-MYH11* (n = 2), *MLL* rearranged (n = 3), *PML-RARA* (n = 2), *NUP98-NSD1* (n = 2), *HLXB9-ETV6* (n = 1), and AML cases lacking chimeric genes (n = 11). Please see Supplemental Experimental Procedures for further details.

FISH

Dual-color FISH was performed on archived bone marrow cells and cell lines as described previously by Mullighan et al. (2007). Probes were derived from bacterial artificial chromosome (BAC) clones (Invitrogen). BACs used were RP11-830F9 (*CBFA2T3*), CTD-25555M20 (*GLIS2*), RP11-345E21 (*MN1*), and CTD-2542E23 (*FLI1*). BAC clone identity was verified by T7 and SP6 BAC-end sequencing and by hybridization of fluorescently labeled BAC DNA with normal human metaphase preparations.

Cloning of *CBFA2T3-GLIS2* and *GLIS2*

Total RNA was extracted from leukemia blasts using RNeasy (QIAGEN) and reverse transcribed using Superscript III (Invitrogen) as per manufacturer's instructions. The coding region of *CBFA2T3-GLIS2* was PCR amplified from patient M712 and M707 using primers *CBFA2T3_119F* and *GLIS2_1685R* (see Supplemental Experimental Procedures for primers and conditions). *GLIS2* was PCR amplified from cDNA using primers *GLIS2_21F* and *GLIS2_1685R* (see Supplemental Experimental Procedures for primers and conditions). PCR products were subcloned into the pGEM-T Easy Vector (Promega) and sequenced. Clones containing the correct sequence were then subcloned into the MIC retroviral backbone (Volanakis et al., 2009).

Murine Bone Marrow Transduction and Colony-Forming Assays

All experiments involving mice were reviewed and approved by the Institutional Animal Care and Use Committee. Bone marrow from 4- to 6-week-old female C57/BL6 mice was harvested and cultured in the presence of recombinant murine SCF (rmSCF), IL3 (rmIL3), and IL6 (rmIL6) (Peprotech; all 50 ng/ml) for 24 hr prior to transduction on RetroNectin (Takara Bio)-coated plates. Eco-tropic envelope-pseudotyped retroviral supernatant was produced by transient transfection of 293T cells as previously described by Soneoka et al. (1995). Forty-eight hours following transduction, cells were harvested, sorted for mCherry expression, and plated on methylcellulose containing IL3, IL6, SCF, and EPO (Stem Cell Technologies, Vancouver, British Columbia, Canada) as per manufacturer's instructions. Colonies were counted after 7 days of growth at 37°C, harvested, and replated. In a subset of experiments, dorsomorphin (Sigma-Aldrich) was added to the methylcellulose at the indicated concentrations.

Flow Cytometry

Cells were resuspended in PBS and preincubated with anti-CD16/CD32 Fc-block (BD PharMingen) if staining did not include conjugated anti-murine CD16/32. Aliquots were stained for 15 min at 4°C with conjugated antibodies. Cells were washed and resuspended in DAPI containing solution (1 µg/ml DAPI in PBS) for subsequent analysis using FACS LSR II D (BD Biosciences). For a list of antibodies used, please see Supplemental Experimental Procedures.

Luciferase Assays

The human BMP4 promoter-driven luciferase construct pSLA4.1EX (Van den Wijngaard et al., 1999) was kindly provided by E. Joop van Zoelen, Nijmegen, The Netherlands. The murine BMP response element (pBRE) (Korchynskyi and ten Dijke, 2002) was kindly provided by Peter ten Dijke, Leiden, The Netherlands. The 8 × 3' Gli-BS luciferase reporter (pGli-BS) (Sasaki et al., 1997) has been previously described. TOPFlash and FOPFlash (Korinek et al., 1997) constructs were obtained from Addgene. For details on luciferase reporter assays, please see Supplemental Experimental Procedures.

ELISA

BMP4 protein levels in the supernatants from transduced murine hematopoietic cells were determined by ELISA. Briefly, mCherry-positive bone marrow cells transduced with empty (MIC), GLIS2, or CBFA2T3-GLIS2-containing retroviruses were placed in media containing IL3, IL6, and SCF for 48 hr, and supernatant was then harvested and the level of murine BMP4 determined using an ELISA kit purchased from TSZELISA (<http://www.tszelisa.com>). Measurements were done according to manufacturer's instructions.

Transgenic *Drosophila*

CBFA2T3-GLIS2 and GLIS2 cDNAs were subcloned into the *pUAS-attB* plasmid (Bischof et al., 2007). Transgenic UAS-CBFA2T3-GLIS2 and UAS-GLIS2 flies were generated using site-specific ϕ C31 integration system (Bischof et al., 2007). Embryo injections were performed by Best Gene. UAS constructs were targeted to chromosome 2R-51D in order to avoid differential positional effects on transgene expression. For wing imaginal disc staining, relevant crosses were performed to generate flies carrying all three transgenes: *Apterous-Gal4* (a strong epithelial dorsal compartment-specific GAL4 driver), UAS-CBFA2T3-GLIS2, and a *dpp-lacZ* enhancer trap reporter. Gal4 driver and *dpp-lacZ* reporter stocks were obtained from the Bloomington Stock Center. Wing imaginal discs were dissected from wandering third-instar larvae, fixed, and immunostained using anti- β -gal (Promega; Z378), anti-CBFA2T3 (Abcam; ab33072), and DAPI (Invitrogen; D3571) as previously described by Carroll et al. (2012). To assess the phenotypic effects of CBFA2T3-GLIS2 and GLIS2, UAS transgenes were expressed under control of the epithelial driver *C765-Gal4*, and progeny was observed. Pharate adults were dissected from pupal casings and imaged.

ACCESSION NUMBERS

The sequence data and SNP microarray data have been deposited in the dbGaP database (<http://www.ncbi.nlm.nih.gov/gap>) under the accession number phs000413.v1.p1. Affymetrix gene expression data have been deposited in the NCBI Gene Expression Omnibus (<http://www.ncbi.nlm.nih.gov/geo/>) under GSE35203.

SUPPLEMENTAL INFORMATION

Supplemental Information includes five figures, seven tables, and Supplemental Experimental Procedures and can be found with this article online at <http://dx.doi.org/10.1016/j.ccr.2012.10.007>.

ACKNOWLEDGMENTS

The authors would like to specifically thank Joy Nakitandwe for critical input and discussions, Susana Raimondi for review of cytogenetics, Matt Stine for assistance with data deposition, Bill Pappas and Scott Malone for support of the information technology infrastructure, and the staff of Tissue Resources Laboratory, Flow Cytometry and Cell Sorting Core, the Hartwell Center for Biotechnology and Bioinformatics of St Jude Children's Research Hospital, and Emily Dolezale for assistance in sample procurement at Memorial Sloan Kettering Cancer Center. This work was supported by grants from the National Institutes of Health (Cancer Center Support Grant P30 CA021765), the Eric Trump Foundation, a Leukemia & Lymphoma Society Specialized Center of Research Grant LLS7015, and the American Lebanese Syrian Associated Charities (ALSAC) of St Jude Children's Research Hospital.

Received: June 21, 2012

Revised: September 5, 2012

Accepted: October 17, 2012

Published: November 12, 2012

REFERENCES

Argiropoulos, B., and Humphries, R.K. (2007). Hox genes in hematopoiesis and leukemogenesis. *Oncogene* 26, 6766–6776.

Athale, U.H., Razzouk, B.I., Raimondi, S.C., Tong, X., Behm, F.G., Head, D.R., Srivastava, D.K., Rubnitz, J.E., Bowman, L., Pui, C.H., and Ribeiro, R.C. (2001). Biology and outcome of childhood acute megakaryoblastic leukemia: a single institution's experience. *Blood* 97, 3727–3732.

Attanasio, M., Uhlenhaut, N.H., Sousa, V.H., O'Toole, J.F., Otto, E., Anlag, K., Klugmann, C., Treier, A.C., Helou, J., Sayer, J.A., et al. (2007). Loss of GLIS2 causes nephronophthisis in humans and mice by increased apoptosis and fibrosis. *Nat. Genet.* 39, 1018–1024.

Barakat, M.T., Humke, E.W., and Scott, M.P. (2010). Learning from Jekyll to control Hyde: Hedgehog signaling in development and cancer. *Trends Mol. Med.* 16, 337–348.

Barnard, D.R., Alonzo, T.A., Gerbing, R.B., Lange, B., and Woods, W.G.; Children's Oncology Group. (2007). Comparison of childhood myelodysplastic syndrome, AML FAB M6 or M7, CCG 2891: report from the Children's Oncology Group. *Pediatr. Blood Cancer* 49, 17–22.

Barretina, J., Caponigro, G., Stransky, N., Venkatesan, K., Margolin, A.A., Kim, S., Wilson, C.J., Lehár, J., Kryukov, G.V., Sonkin, D., et al. (2012). The Cancer Cell Line Encyclopedia enables predictive modelling of anticancer drug sensitivity. *Nature* 483, 603–607.

Bhardwaj, G., Murdoch, B., Wu, D., Baker, D.P., Williams, K.P., Chadwick, K., Ling, L.E., Karanu, F.N., and Bhatia, M. (2001). Sonic hedgehog induces the proliferation of primitive human hematopoietic cells via BMP regulation. *Nat. Immunol.* 2, 172–180.

Bhatia, M., Bonnet, D., Wu, D., Murdoch, B., Wrana, J., Gallacher, L., and Dick, J.E. (1999). Bone morphogenetic proteins regulate the developmental program of human hematopoietic stem cells. *J. Exp. Med.* 189, 1139–1148.

Bischof, J., Maeda, R.K., Hediger, M., Karch, F., and Basler, K. (2007). An optimized transgenesis system for *Drosophila* using germ-line-specific ϕ C31 integrases. *Proc. Natl. Acad. Sci. USA* 104, 3312–3317.

Buijs, A., van Rompaey, L., Molijn, A.C., Davis, J.N., Vertegaal, A.C., Potter, M.D., Adams, C., van Baal, S., Zwarthoff, E.C., Roussel, M.F., and Grosveld, G.C. (2000). The MN1-TEL fusion protein, encoded by the translocation (12;22)(p13;q11) in myeloid leukemia, is a transcription factor with transforming activity. *Mol. Cell. Biol.* 20, 9281–9293.

Carroll, A., Civin, C., Schneider, N., Dahl, G., Pappo, A., Bowman, P., Emami, A., Gross, S., Alvarado, C., Phillips, C., et al. (1991). The t(1;22) (p13;q13) is nonrandom and restricted to infants with acute megakaryoblastic leukemia: a Pediatric Oncology Group Study. *Blood* 78, 748–752.

Carroll, C.E., Marada, S., Stewart, D.P., Ouyang, J.X., and Ogden, S.K. (2012). The extracellular loops of Smoothened play a regulatory role in control of Hedgehog pathway activation. *Development* 139, 612–621.

Chyla, B.J., Moreno-Miralles, I., Steapleton, M.A., Thompson, M.A., Bhaskara, S., Engel, M., and Hiebert, S.W. (2008). Deletion of Mtg16, a target of t(16;21), alters hematopoietic progenitor cell proliferation and lineage allocation. *Mol. Cell. Biol.* 28, 6234–6247.

Creutzig, U., Reinhardt, D., Diekamp, S., Dworzak, M., Stary, J., and Zimmermann, M. (2005). AML patients with Down syndrome have a high cure rate with AML-BFM therapy with reduced dose intensity. *Leukemia* 19, 1355–1360.

Dahn, R.D., and Fallon, J.F. (2000). Interdigital regulation of digit identity and homeotic transformation by modulated BMP signaling. *Science* 289, 438–441.

Downing, J.R., Wilson, R.K., Zhang, J., Mardis, E.R., Pui, C.-H., Ding, L., Ley, T.J., and Evans, W.E. (2012). The Pediatric Cancer Genome Project. *Nat. Genet.* 44, 619–622.

Fuchs, O., Simakova, O., Klener, P., Cmejlova, J., Zivny, J., Zavadil, J., and Stopka, T. (2002). Inhibition of Smad5 in human hematopoietic progenitors blocks erythroid differentiation induced by BMP4. *Blood Cells Mol. Dis.* 28, 221–233.

Gamou, T., Kitamura, E., Hosoda, F., Shimizu, K., Shinohara, K., Hayashi, Y., Nagase, T., Yokoyama, Y., and Ohki, M. (1998). The partner gene of AML1 in t(16;21) myeloid malignancies is a novel member of the MTG8(ETO) family. *Blood* 91, 4028–4037.

- Grieder, N.C., Morata, G., Affolter, M., and Gehring, W.J. (2009). Spalt major controls the development of the notum and of wing hinge primordia of the *Drosophila melanogaster* wing imaginal disc. *Dev. Biol.* 329, 315–326.
- Heuser, M., Yun, H., Berg, T., Yung, E., Argiropoulos, B., Kuchenbauer, F., Park, G., Hamwi, I., Palmqvist, L., Lai, C.K., et al. (2011). Cell of origin in AML: susceptibility to MN1-induced transformation is regulated by the MEIS1/AbdB-like HOX protein complex. *Cancer Cell* 20, 39–52.
- Higuchi, M., O'Brien, D., Kumaravelu, P., Lenny, N., Yeoh, E.J., and Downing, J.R. (2002). Expression of a conditional AML1-ETO oncogene bypasses embryonic lethality and establishes a murine model of human t(8;21) acute myeloid leukemia. *Cancer Cell* 1, 63–74.
- Hui, C.C., and Angers, S. (2011). Gli proteins in development and disease. *Annu. Rev. Cell Dev. Biol.* 27, 513–537.
- Iafate, A.J., Feuk, L., Rivera, M.N., Listewnik, M.L., Donahoe, P.K., Qi, Y., Scherer, S.W., and Lee, C. (2004). Detection of large-scale variation in the human genome. *Nat. Genet.* 36, 949–951.
- Ingham, P.W., and McMahon, A.P. (2001). Hedgehog signaling in animal development: paradigms and principles. *Genes Dev.* 15, 3059–3087.
- Jeanpierre, S., Nicolini, F.E., Kaniowski, B., Dumontet, C., Rimokh, R., Puisieux, A., and Maguer-Satta, V. (2008). BMP4 regulation of human megakaryocytic differentiation is involved in thrombopoietin signaling. *Blood* 112, 3154–3163.
- Kawada, H., Ito, T., Pharr, P.N., Spyropoulos, D.D., Watson, D.K., and Ogawa, M. (2001). Defective megakaryopoiesis and abnormal erythroid development in Fli-1 gene-targeted mice. *Int. J. Hematol.* 73, 463–468.
- Kim, Y.S., Kang, H.S., and Jetten, A.M. (2007). The Krüppel-like zinc finger protein Glis2 functions as a negative modulator of the Wnt/beta-catenin signaling pathway. *FEBS Lett.* 581, 858–864.
- Korchynski, O., and ten Dijke, P. (2002). Identification and functional characterization of distinct critically important bone morphogenetic protein-specific response elements in the Id1 promoter. *J. Biol. Chem.* 277, 4883–4891.
- Korinek, V., Barker, N., Morin, P.J., van Wichen, D., de Weger, R., Kinzler, K.W., Vogelstein, B., and Clevers, H. (1997). Constitutive transcriptional activation by a beta-catenin-Tcf complex in APC-/- colon carcinoma. *Science* 275, 1784–1787.
- Krzywinski, M., Schein, J., Birol, I., Connors, J., Gascoyne, R., Horsman, D., Jones, S.J., and Marra, M.A. (2009). Circos: an information aesthetic for comparative genomics. *Genome Res.* 19, 1639–1645.
- Lamar, E., Kintner, C., and Goulding, M. (2001). Identification of NKL, a novel Gli-Krüppel zinc-finger protein that promotes neuronal differentiation. *Development* 128, 1335–1346.
- Lim, Y., and Matsui, W. (2010). Hedgehog signaling in hematopoiesis. *Crit. Rev. Eukaryot. Gene Expr.* 20, 129–139.
- Lin, M., Wei, L.J., Sellers, W.R., Lieberfarb, M., Wong, W.H., and Li, C. (2004). dChipSNP: significance curve and clustering of SNP-array-based loss-of-heterozygosity data. *Bioinformatics* 20, 1233–1240.
- Lion, T., Haas, O.A., Harbott, J., Bannier, E., Ritterbach, J., Jankovic, M., Fink, F.M., Stojimirovic, A., Herrmann, J., Riehm, H.J., et al. (1992). The translocation t(1;22)(p13;q13) is a nonrandom marker specifically associated with acute megakaryocytic leukemia in young children. *Blood* 79, 3325–3330.
- Ma, Z., Morris, S.W., Valentine, V., Li, M., Herbrick, J.A., Cui, X., Bouman, D., Li, Y., Mehta, P.K., Nizetic, D., et al. (2001). Fusion of two novel genes, RBM15 and MKL1, in the t(1;22)(p13;q13) of acute megakaryoblastic leukemia. *Nat. Genet.* 28, 220–221.
- Malinge, S., Ragu, C., Della-Valle, V., Pisani, D., Constantinescu, S.N., Perez, C., Villeval, J.L., Reinhardt, D., Landman-Parker, J., Michaux, L., et al. (2008). Activating mutations in human acute megakaryoblastic leukemia. *Blood* 112, 4220–4226.
- Mardis, E.R., Ding, L., Dooling, D.J., Larson, D.E., McLellan, M.D., Chen, K., Koboldt, D.C., Fulton, R.S., Delehaunty, K.D., McGrath, S.D., et al. (2009). Recurring mutations found by sequencing an acute myeloid leukemia genome. *N. Engl. J. Med.* 361, 1058–1066.
- McCarroll, S.A., Kuruvilla, F.G., Korn, J.M., Cawley, S., Nemesh, J., Wysoker, A., Shaper, M.H., de Bakker, P.I., Maller, J.B., Kirby, A., et al. (2008). Integrated detection and population-genetic analysis of SNPs and copy number variation. *Nat. Genet.* 40, 1166–1174.
- Mercher, T., Coniat, M.B., Monni, R., Mauchauffe, M., Nguyen Khac, F., Gressin, L., Mugneret, F., Leblanc, T., Dastugue, N., Berger, R., and Bernard, O.A. (2001). Involvement of a human gene related to the *Drosophila* spen gene in the recurrent t(1;22) translocation of acute megakaryocytic leukemia. *Proc. Natl. Acad. Sci. USA* 98, 5776–5779.
- Mullighan, C.G., Goorha, S., Radtke, I., Miller, C.B., Coustan-Smith, E., Dalton, J.D., Girtman, K., Mathew, S., Ma, J., Pounds, S.B., et al. (2007). Genome-wide analysis of genetic alterations in acute lymphoblastic leukaemia. *Nature* 446, 758–764.
- Oki, Y., Kantarjian, H.M., Zhou, X., Cortes, J., Faderl, S., Verstovsek, S., O'Brien, S., Koller, C., Beran, M., Bekele, B.N., et al. (2006). Adult acute megakaryocytic leukemia: an analysis of 37 patients treated at M.D. Anderson Cancer Center. *Blood* 107, 880–884.
- Olshen, A.B., Venkatraman, E.S., Lucito, R., and Wigler, M. (2004). Circular binary segmentation for the analysis of array-based DNA copy number data. *Biostatistics* 5, 557–572.
- Pounds, S., Cheng, C., Mullighan, C., Raimondi, S.C., Shurtleff, S., and Downing, J.R. (2009). Reference alignment of SNP microarray signals for copy number analysis of tumors. *Bioinformatics* 25, 315–321.
- Radtke, I., Mullighan, C.G., Ishii, M., Su, X., Cheng, J., Ma, J., Ganti, R., Cai, Z., Goorha, S., Pounds, S.B., et al. (2009). Genomic analysis reveals few genetic alterations in pediatric acute myeloid leukemia. *Proc. Natl. Acad. Sci. USA* 106, 12944–12949.
- Sander, V., Eivers, E., Choi, R.H., and De Robertis, E.M. (2010). *Drosophila* Smad2 opposes Mad signaling during wing vein development. *PLoS One* 5, e10383.
- Sasaki, H., Hui, C., Nakafuku, M., and Kondoh, H. (1997). A binding site for Gli proteins is essential for HNF-3beta floor plate enhancer activity in transgenics and can respond to Shh in vitro. *Development* 124, 1313–1322.
- Söderberg, S.S., Karlsson, G., and Karlsson, S. (2009). Complex and context dependent regulation of hematopoiesis by TGF-beta superfamily signaling. *Ann. N Y Acad. Sci.* 1176, 55–69.
- Soneoka, Y., Cannon, P.M., Ramsdale, E.E., Griffiths, J.C., Romano, G., Kingsman, S.M., and Kingsman, A.J. (1995). A transient three-plasmid expression system for the production of high titer retroviral vectors. *Nucleic Acids Res.* 23, 628–633.
- Tabata, T., and Takei, Y. (2004). Morphogens, their identification and regulation. *Development* 131, 703–712.
- Tallman, M.S., Neuberg, D., Bennett, J.M., Francois, C.J., Paietta, E., Wiernik, P.H., Dewald, G., Cassileth, P.A., Oken, M.M., and Rowe, J.M. (2000). Acute megakaryocytic leukemia: the Eastern Cooperative Oncology Group experience. *Blood* 96, 2405–2411.
- Van den Wijngaard, A., Pijpers, M.A., Joosten, P.H., Roelofs, J.M., Van zoelen, E.J., and Olijve, W. (1999). Functional characterization of two promoters in the human bone morphogenetic protein-4 gene. *J. Bone Miner. Res.* 14, 1432–1441.
- Visvader, J.E., Crossley, M., Hill, J., Orkin, S.H., and Adams, J.M. (1995). The C-terminal zinc finger of GATA-1 or GATA-2 is sufficient to induce megakaryocytic differentiation of an early myeloid cell line. *Mol. Cell. Biol.* 15, 634–641.
- Vokes, S.A., Ji, H., McCuine, S., Tenzen, T., Giles, S., Zhong, S., Longabaugh, W.J., Davidson, E.H., Wong, W.H., and McMahon, A.P. (2007). Genomic characterization of Gli-activator targets in sonic hedgehog-mediated neural patterning. *Development* 134, 1977–1989.
- Volanakis, E.J., Williams, R.T., and Sherr, C.J. (2009). Stage-specific Arf tumor suppression in Notch1-induced T-cell acute lymphoblastic leukemia. *Blood* 114, 4451–4459.
- Wang, G.G., Song, J., Wang, Z., Dormann, H.L., Casadio, F., Li, H., Luo, J.L., Patel, D.J., and Allis, C.D. (2009). Haematopoietic malignancies caused by dysregulation of a chromatin-binding PHD finger. *Nature* 459, 847–851.

Wang, L., Gural, A., Sun, X.J., Zhao, X., Perna, F., Huang, G., Hatlen, M.A., Vu, L., Liu, F., Xu, H., et al. (2011). The leukemogenicity of AML1-ETO is dependent on site-specific lysine acetylation. *Science* 333, 765–769.

Yu, P.B., Hong, C.C., Sachidanandan, C., Babbitt, J.L., Deng, D.Y., Hoyng, S.A., Lin, H.Y., Bloch, K.D., and Peterson, R.T. (2008). Dorsomorphin inhibits BMP signals required for embryogenesis and iron metabolism. *Nat. Chem. Biol.* 4, 33–41.

Zhang, J., Wheeler, D.A., Yakub, I., Wei, S., Sood, R., Rowe, W., Liu, P.P., Gibbs, R.A., and Buetow, K.H. (2005). SNPdetector: a software tool for sensitive and accurate SNP detection. *PLoS Comput. Biol.* 1, e53.

Zhang, J., Ding, L., Holmfeldt, L., Wu, G., Heatley, S.L., Payne-Turner, D., Easton, J., Chen, X., Wang, J., Rusch, M., et al. (2012). The genetic basis of early T-cell precursor acute lymphoblastic leukaemia. *Nature* 481, 157–163.